FPCM-9 (2008)
The 9th International Conference on Flow Processes in Composite Materials
Montréal (Québec), Canada
8 ~ 10 July 2008

MESOSCALE SIMULATION OF THE FLOW OF NON-NEWTONIAN FLUIDS THROUGH SHEARED TEXTILE REINFORCEMENTS

F. Loix [1], P. Badel [2], L. Orgéas [1, 4], C. Geindreau [1], P. Boisse [2], J.-F. Bloch [3]

[1] *CNRS / Université de Grenoble, Laboratoire Sols-Solides-Structures-Risques (3SR), BP 53, 38041 Grenoble cedex 9, France*
[2] *Laboratoire de Mécanique des Contacts et des Structures (LaMCoS), CNRS / INSA Lyon, Bâtiment Jacquard, F-69621 Villeurbanne cedex, France*
[3] *CNRS / Université de Grenoble, Laboratoire de Génie des Procédés Papetiers (LGP2), BP 65, 461 rue de la Papeterie, 38402 Saint-Martin-d'Hères cedex, France*
[4] *Corresponding author's Email: Laurent.Orgeas@hmg.inpg.fr*

SUMMARY: A three steps method is proposed to compute the flow of viscous fluids through deformed textile reinforcements. In the first step, In the first step, the in-plane shear of a dry plain,weave before and after the shear locking is simulated at the mescoscale on Representative Elementary Volumes (REV's) of the periodic plain weave, accounting for bundle-bundle contacts and large transformations, and assuming that bundles behave as transversely isotropic hypoelastic materials. The second step consists in simulating the mesoscale flow of viscous fluids through the as-deformed solid REV's in order to determine in the third step the macroscopic flow law. For Newtonian fluids, numerical results emphasize the drastic changes of the permeability tensor as the plain weave is sheared: loss of transverse isotropy and non trivial evolution of the components of the permeability tensor. The influence of the flowing fluid rheology is also emphasized in case of generalized Newtonian fluids. For these fluids, a method is then proposed to formulate the macroscopic flow law, within the framework of the theory of anisotropic tensor functions and by using mechanical iso-dissipation curves.

KEYWORDS: shear deformation, textile reinforcement, permeability, non-Newtonian flow, meso-macro analysis, computational analysis

INTRODUCTION

It is essential to accurately predict polymer flows in woven or non-woven fiber preforms for a number of liquid molding processes [1], among which the Resin Transfer Molding process (RTM). Nevertheless, the determination with a high precision of the flow description still remains difficult. Textiles' manufacturers can provide a material property list which sometimes contains the permeability of fabrics, usually measured when fabrics are not deformed:

- During the performing stage of RTM woven fabrics undergo mechanical loadings which can induce very large deformations of the textiles of which dominant mode is the shear deformation [2]. This affects their permeability and has to be understood and quantified.
- The permeability is a property that is only dedicated to the flow of Newtonian fluids through porous media. However, liquid polymers may exhibit non-Newtonian behavior (thermoset polymers as they are curing or thermoplastic polymers with long polymer chains), especially at the high shear rates they may be subjected when they flow through networks of fibers. Under such circumstances, their flow through woven or non-woven textile reinforcements may be complex and may severely deviates from that of Newtonian fluids [3-6].

Within that context, a method is proposed in this work in order to determine the macroscopic flow law for non-Newtonian fluids flowing through highly deformed textile reinforcements. The method is illustrated here with a periodic woven fabric. It is divided in three steps. Firstly, the in-plane shear of a dry plain weave before and after the shear locking is studied from a mesoscale analysis achieved with a Representative Elementary Volume (REV) of the periodic textile. The second step consists in simulating the mesoscale flow through the as-deformed solid REV's in order to study the flow of the polymer through the woven fabrics. Numerical results emphasized the drastic changes of the permeation law when the considered plain weave fabric was sheared, such as its loss of transverse isotropy. The influence of the flowing fluid rheology is also emphasized in the case of power-law fluids. In the third a last step, a method is proposed to formulate the macroscopic flow law, within the framework of the theory of anisotropic tensor functions and using mechanical iso-dissipation curves.

STEP 1 – PREDEFORMATION OF THE TEXTILE

We have considered here quite simple textile reinforcement. It is a periodic glass plain weave which is balanced since the warp and the weft bundles have identical geometrical and mechanical properties. Its geometry is based on circle arcs and tangent segments. It is simple but ensures consistency of the model, which means that bundles do not penetrate each other [7]. A scheme of the periodic solid REV of such a mesostructure is given in Fig. 1a.

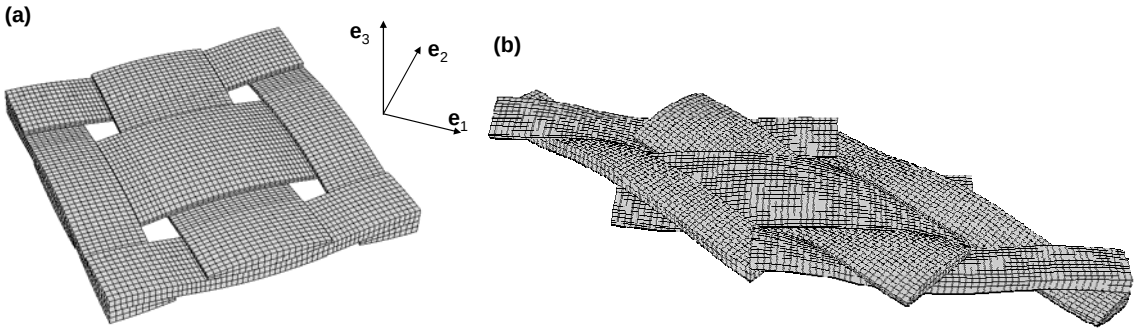

Fig. 1 Solid REV of the studied plain weave: geometry and FE mesh before deformation (a) and after a pre-shear angle of 53° in the ($\mathbf{e}_1$, $\mathbf{e}_2$) plane (b).

As extensively described in [2], this solid REV was subjected to a significant in-plane shear. In order to compute its corresponding deformed shape, finite elements calculations were performed with the commercial FE code Abaqus. Briefly, the following assumptions were stated to run the simulation:

- Very large transformations were taken into account.
- Consistent bundle-bundle contacts were assumed to induce Coulomb friction forces (dry friction coefficient $f = 0.2$)
- Fiber bundles were assumed to behave like transversely isotropic hypoelastic continua, which symmetry direction is locally parallel to the direction of fibers within the bundles. Hence, their mechanical behavior is given by the following constitutive relation:

$$\boldsymbol{\sigma}^{\nabla} = \mathbf{C} : \mathbf{D} \qquad (1)$$

  where $\mathbf{C}$ is the fourth order incremental stiffness tensor (requiring 5 constitutive parameters, *i.e.* longitudinal E_l, ν_l and transverse E_t, ν_t Young moduli and Poisson ratios, and a shear modulus G), $\mathbf{D}$ is the second order strain rate tensor and $\boldsymbol{\sigma}^{\nabla}$ is an objective derivative of the second order Cauchy stress tensor $\boldsymbol{\sigma}$. Such a derivative is computed by following the local rotation of fibers during the macroscopic shearing [2].
- Calculations were achieved by subjecting the whole solid REV to a mean macroscopic displacement gradient corresponding to an in-plane shear. Thereby, the periodic fluctuations of the displacement required to accommodate the imposed mechanical loading were computed. This allows determining the deformed shape of the solid REV's.

As an example, Fig. 1b give the deformed shape of the solid REV after an imposed shear angle of 53°, *i.e.* largely above the locking angle [2].

STEP 2 – FLUID FLOW MESOSCALE SIMULATION

From the as-deformed solid REV's, associated fluid REV's were then built in order to study the flow of the polymer through them [8]. Briefly, solid REV's obtained with the FE code Abaqus are represented by means of meshes for each individual yarn. Those meshes have first to be transformed in solid entities which are then assembled. Once a unique solid entity is obtained, it must be subtracted from a well-chosen volume to give the fluid REV. Keeping same periods as the solid ones would generate difficulties to construct the corresponding fluid REV's. The fluid period has then been adapted in a appropriate way to easily impose periodic boundary conditions (see Fig. 2, [8]).

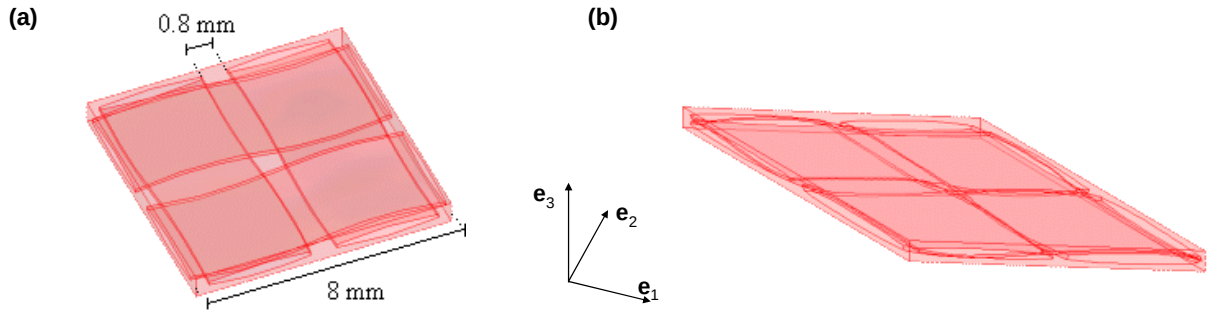

Fig. 2 Fluid REV's corresponding to the solid REV's sketched in Fig. 1.

Therefrom, the mescocale slow flow of a generalized Newtonian fluid through the as-deformed solid REV's was analyzed [9] by using an upscaling technique, namely the homogenization method with multiple scale asymptotic expansion [10-12]. Hence, by assuming sticking boundary conditions at the fluid solid interfaces, the following fluid flow problem deduced from the upscaling process was solved within the fluid REV's:

$$\begin{cases} \nabla \cdot \overline{\mathbf{v}} = 0 \\ 2\nabla \cdot \left(\mu(\dot{\overline{\gamma}})\, \overline{\mathbf{D}} \right) = \nabla \varepsilon p + \nabla \overline{p} \end{cases} \tag{2}$$

where the so-called first order pressure gradient $\nabla \overline{p}$ is constant and given in the entire fluid REV's, and where the first order velocity field $\overline{\mathbf{v}}$ as well as the fluctuation pressure εp are the periodic unknowns. Notice that the shear viscosity of the fluid μ which is involved in (2) is a convex function of the generalized shear rate $\dot{\overline{\gamma}} = \sqrt{2\overline{\mathbf{D}} : \overline{\mathbf{D}}}$. Hence, a large class of rheological models can be taken into account in the present multiscale approach: Newtonian fluids (constant viscosity) [8], power-law fluids [5-6], Carreau-Yasuda fluids [9], regularized versions of the Bingham or the Herschel–Bulkley fluids, In this work, for the sake of simplicity, we have considered here a power-law fluid, which viscosity μ is simply expressed as:

$$\mu = \mu_0 \dot{\gamma}^{n-1}, \tag{3}$$

μ_0 being the consistency and n the strain rate sensitivity. Within given shear rate ranges, such a model usually allows rather good fits of the steady state shear viscosities of thermoplastic or thermoset liquid polymers. Lastly, notice that the well-posed boundary value problem (2) was solved with a mixt pressure-velocity formulation implemented in the finite element commercial code Comsol, by using tetrahedral P2-P1 finite elements.

STEP 3 – STUDY OF THE MACROSCOPIC FLOW LAW

The macroscopic description corresponding to the above mesoscale fluid flow problem is expressed by the following macroscopic mass and momentum balance equations:

$$\begin{cases} \nabla \cdot \langle \overline{\mathbf{v}} \rangle = 0 \\ \nabla \overline{p} = \mathbf{f}(\mu_0, n, mesosctructure) \end{cases} \tag{4}$$

where the macroscopic velocity field $\langle \overline{\mathbf{v}} \rangle$ is the volume average of the mesoscopic velocity field $\overline{\mathbf{v}}$, and where $\mathbf{f}$ is a volumetric viscous drag force. This is directly deduced from the upscaling process, without *a priori* assumption at the macroscale [9].

In the case of a Newtonian fluid, *i.e.* when $\mu = \mu_0 = \text{cst}$ ($n = 1$), (4b) reduces to the well-known Darcy's law since

$$\mathbf{f} = -\mu_0\, \mathbf{K}^{-1} \cdot \langle \overline{\mathbf{v}} \rangle, \tag{5}$$

where $\mathbf{K}$ is the permeability tensor.

For other generalized Newtonian fluid, the Darcy's law is not valid any more. However, **f** can be expressed as the gradient of a viscous dissipation potential $\langle\Phi\rangle$ with respect to the macroscopic velocity field $\langle\overline{\mathbf{v}}\rangle$ [6,9]. In case of a power-law flowing fluid, this yields:

$$\mathbf{f} = -\frac{\partial\langle\Phi\rangle}{\partial\langle\overline{\mathbf{v}}\rangle} = -\frac{\mu_0}{l_c}\left(\frac{v_{eq}}{\phi\, l_c}\right)^n \frac{\partial\, v_{eq}}{\partial\langle\overline{\mathbf{v}}\rangle} \tag{6}$$

where l_c is the characteristic length of sheared fluid at the mesoscale, ϕ can be defined as the "active" volume fraction of pores effectively contributing to the flow [8]: they can be obtained by simulating and analyzing the flow in the $\mathbf{e}_1$ direction. The positive scalar v_{eq} also appearing in the last equation is an equivalent macroscopic velocity: any iso-equivalent velocity surface (iso-v_{eq}) plotted in the velocity space corresponds to an iso-dissipation surface and to an iso-potential surface (iso-$\langle\Phi\rangle$). Fitting with a suitable phenomenological form numerical iso-v_{eq} surfaces deduced from mesoscale simulations allows obtaining the whole macroscopic flow law. In accordance with (6), notice that the volumetric viscous drag force **f** is normal to the iso-v_{eq} surfaces. For the mesoscopic flow law exhibiting orthotropy (see next section), the following continuous form of v_{eq} is proposed [9]:

$$v_{eq}{}^m = v_{eqa}{}^m + v_{eqb}{}^m, \tag{7}$$

with

$$\begin{cases} v_{eqa}{}^{m_a} = V_I{}^{m_a} + \left(V_{II}/A\right)^{m_a} \\ v_{eqb} = V_{III}/B \\ m = \left(m_b V_I{}^2 + m_c V_{II}{}^2\right)/\left(V_I{}^2 + V_{II}{}^2\right) \end{cases}, \tag{8}$$

It involves velocity invariants V_i defined as:

$$V_i = \sqrt{\langle\overline{\mathbf{v}}\rangle\cdot(\mathbf{e}_i\otimes\mathbf{e}_i)\cdot\langle\overline{\mathbf{v}}\rangle},\ i = I, II, III\ \ (\text{no summation}), \tag{8}$$

where the $\mathbf{e}_i$'s ($i = I, II, III$) are the orthogonal principal unit vectors of the macroscopic flow law. This form also involves five additional constitutive parameters:

- A and B can be directly deduced from the mesoscale simulation of the flow along the $\mathbf{e}_{II}$ and $\mathbf{e}_{III}$ directions, respectively. They characterize the magnitude of the anisotropy along the principal directions (see Fig. 4d).
- Curvature parameters m_a, m_b and m_c are chosen to fit the above continuous iso-v_{eq} surfaces to numerical ones. They equal 2 in case of Newtonian flowing fluids.

APPLICATION TO THE PLAIN WEAVE

The above methodology was achieved on the non deformed and sheared plain weaves, such as those sketched in Fig. 2. A first set of simulations was obtained by considering a Newtonian flowing fluid [8]. Two types of boundary conditions were used, *i.e.* full 3D periodicity and 2D in-plane periodicity + sticking boundary conditions at $x_3 = \pm h/2$, h being the thickness of the plane weave. Results have been sketched in Fig. 3. The graph of Fig. 3a represents the evolution, in the reference frame ($\mathbf{e}_1$,$\mathbf{e}_2$,$\mathbf{e}_3$) (which corresponds to the principal reference frame ($\mathbf{e}_I$,$\mathbf{e}_{II}$,$\mathbf{e}_{III}$)), of the

components K_{11}, K_{22} and K_{33} of the permeability tensor **K** expressed as functions of the imposed shear angle. The graph plotted in Fig. 3b gives the evolution of the permeability ratios K_{22} / K_{11} and K_{33} / K_{11} as functions of the imposed shear angle. These two graphs bring up the following comments [8]:

- The non-deformed plain weave displays transverse isotropy ($K_{11} = K_{22} \neq K_{33}$). By contrast, as soon as it is sheared, it exhibits orthotropy ($K_{11} \neq K_{22} \neq K_{33}$). K_{22} undergoes a monotonous decrease with the shear angle. K_{11} increases and K_{33} is nearly constant for angles ranging from 0° to 30°. For larger shear angles, the two latter components decrease.
- By comparing permeabilities between the extreme configurations, K_{11} and K_{22} are found to decrease by a ratio 2 and K_{33} with a ratio 10. Notice that the trend recorded for K_{11} is experimentally retrieved by Smith et al. [13] who used plain-weave fabrics. Hammami et al. [14] performed experiments till 30° on JBMartin NCS fabric and also retrieved the same trend for K_{11} and for K_{22}. The complex trends emphasized in Fig. 3a are ascribed to changes of both the porosity and the morphology of the plain weave during the shearing of the plain weave [8]. Such changes are induced by two closely coupled deformation meso-mechanisms: the relative motions of tows and their intrinsic deformation. For instance, the drastic decrease of K_{33}, which is probably due to the locking of the holes perpendicular to the $\mathbf{e}_3$ direction, is induced both by the relative rotation of tows and their lateral crushing in the vicinities of contact zones (see Fig. 1).
- The evolution of permeability ratios with respect to the shear angle again highlights the loss of in-plane permeability isotropy when the fabric is sheared. We observe a decrease of K_{22} / K_{11} and K_{33} / K_{11}. This trend is also retrieved by Lai and Young [15] and Slade et al [16].
- As shown in Fig. 8a, the evolution of the in-plane permeabilities of a single mat with the shear angle (2D in-plane periodicity) follows the same trend as that observed for the multi-layers preform (3D periodicity). However, they are five times smaller. Moreover, as depicted in Fig. 3b, shearing the single layer reinforcement induces stronger anisotropy than for the multi-layers one.

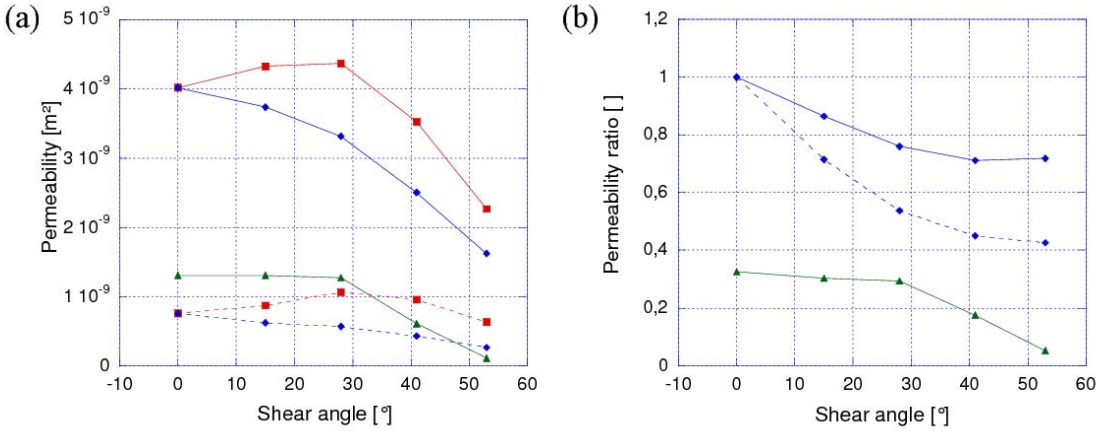

Fig. 3 (a) Computed permeabilities in the principal axes for different imposed shear angles. In continuous lines, a multi-layers configuration is considered while a single layer configuration is studied in dashed lines. Square marks : K_{11}; Diamonds: K_{22} and triangles: K_{33}. (b) Principal permeability ratios K_{22} / K_{11} (diamonds) and K_{33} / K_{11} (triangles) for different imposed shear angles to the woven fabrics.

Then, the proposed expression of v_{eq} was compared to numerical iso-dissipation surfaces obtained from numerical simulation achieved on the REV's shown in Fig. 2, for a Newtonian (n = 1) and a power-law shear thinning fluid (n = 0.3). Results which are given in Fig. 4, conjure up the following comments:

- The numerical iso-dissipation surfaces (stars in Fig. 4) exhibits transverse isotropy for the non-deformed REV and when the fluid is Newtonian (see Fig. 3a and 4a). It is important to notice that such symmetry is broken for the same REV and for a power-law fluid (see Fig. 3b): the macroscopic flow law then exhibits orthotropy. A similar trend was already emphasized when studying the transverse flow of power-law fluids through square arrays of parallel fibers with circular and identical cross sections [6].
- Whatever the fluid considered, shearing the plain weave (i) increase the anisotropy (iso-dissipation surfaces are stretched) and (ii) induce a more difficult flow (iso-dissipation surfaces are smaller). Indeed, compared to the non deformed iso-dissipation surface plotted in Fig. 3b, the iso-dissipation surface obtained for the same fluid but with the sheared REV is (i) flattened in the $\mathbf{e}_3$ direction and (ii) smaller (Fig. 3c).

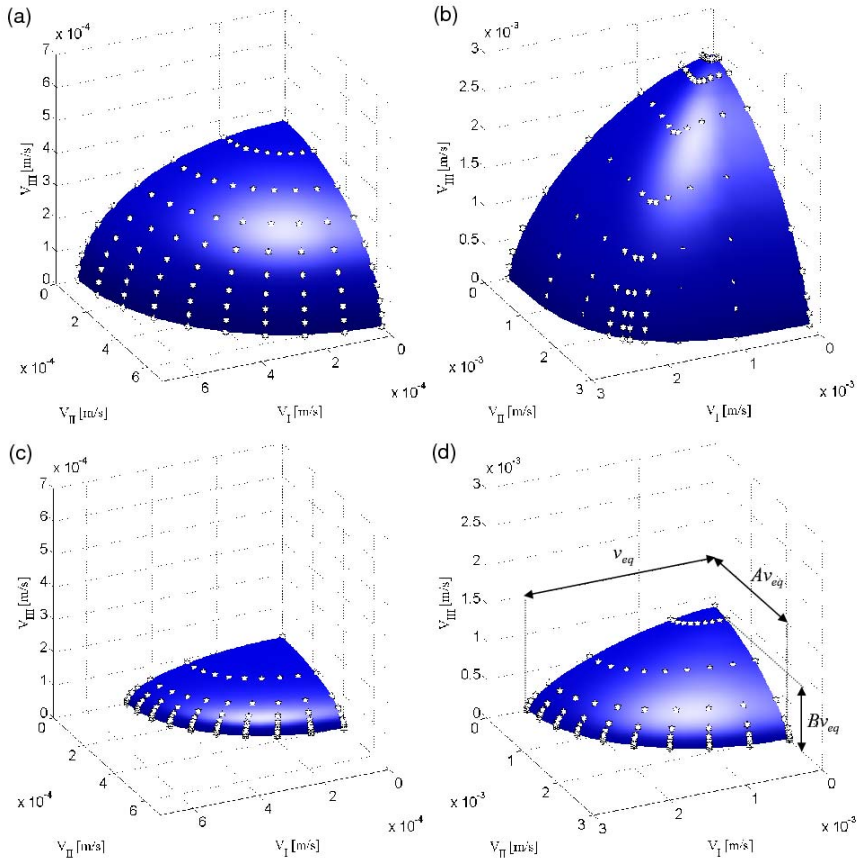

Fig. 4 Numerical (stars) and fitted (continuous surfaces) iso-dissipation surfaces (100 W m^{-3}) plotted in the velocity space and obtained for the non deformed plain weave (a, b) and the 53° shear configuration (c, d), for a Newtonian fluid (μ_0 = 1 Pa s, n = 1) (a, c) and for a power-law shear thinning fluid (μ_0 = 1 Pa s^n, n = 0.3) (b, d). Numerical results (stars) have been determined by solving the localisation problem (3) while the continuous surfaces are modeled by phenomenological equations (7-8).

The format of v_{eq} (continuous surfaces given by (7-8)) allows a nice fit of numerical iso-dissipation surfaces (stars) plotted in the velocity space, whatever the considered textile (non-deformed and sheared) and type of fluid (Newtonian and power-law). Consequently, the method proposed in this work allows obtaining fairly good analytical macroscopic flow law that could be implemented without major difficulties in mould filling software.

CONCLUSION

In this work, we have presented a method in order to investigate the effects of (i) the deformation of textile reinforcements and (ii) the non-Newtonian rheology of polymers on their macroscopic flow law through the considered fabrics. The first step of the method consists in simulating the mesoscale pre-deformation of dry textile REV's. A special attention was paid in order to limit simplifying assumptions that could induce biases on the deformed shape of solid REV's: choice of consistent initial geometry of solid REV's, numerical simulation with large geometrical transformations, appropriate periodic boundary conditions, bundle–bundle mechanical contacts and reasonable hypoelastic model to mimic the intrinsic behavior of fiber bundles. This first step was applied to the in plane shear of a symmetric glass plain weave. The shape of the deformed solid REV seems realistic, even if further efforts are required to improve the quantitative validation of the simulated REV deformed shapes (ongoing work [17]). The second step consists in simulating the mesoscale flow through the as-deformed solid REV's. Despite technical difficulties encountered to obtain suitable fluid REV's from solid ones, numerical results obtained for Newtonian fluids have emphasized the drastic changes of the permeability tensor when the considered plain weave fabric was sheared. The possible non-Newtonian rheology of polymers was also investigated, showing that the macroscopic flow law could also be significantly affected by it. Lastly, the method proposed in [9] to build macroscopic analytical flow law in case of generalized Newtonian fluids was tested and successfully validated in this work. The proposed analytical macroscopic flow law could be implemented without major difficulties in mould filling software.

ACKNOWLEDGEMENTS

Fabrice Loix wish to thank the CNRS for his research grant and the Rhône-Alpes Materials Research Federation / CNRS "FedeRAMS" for its financial support. Pierre Badel also gratefully acknowledges the région Rhône-Alpes via the cluster "MACODEV" for the research grant he benefits.

REFERENCES

1. S.G. Advani "*Flow and Rheology in Polymer Composites Manufacturing*", Elsevier Science, Amsterdam, 1994.

2. P. Badel, E. Vidal Sallé and P. Boisse "Computational determination of inplane shear mechanical behavior of textile composite reinforcements" *Comput. Mater. Sci.* Vol. 40, 2007, pp 439-448.

3. M.V. Bruschke and S.G. Advani "Flow of generalized Newtonian fluids across a periodic array of cylinders" *J. Rheol.* Vol. 37, 1993, pp. 479-498.

4. J.K. Woods, P.D.M. Spelt, P.D. Lee, T. Selerland, C.J. Lawrence, “Creeping flows of power-law fluids through periodic arrays of elliptical cylinders” *J. Non-Newtonian Fluid Mech.* Vol. 111, 2003, pp. 211-228.

5. Z. Idris, L. Orgéas, C Geindreau, J.-F. Bloch, and J.-L. Auriault “Microstructural effects on the flow of power-law fluid through fibrous media” *Modelling Simul. Mater. Sci. Eng.* Vol. 12, 2004, pp. 995-1016.

6. L .Orgéas, Z. Idris, C. Geindreau, J.-F. Bloch, and J.-L. Auriault “Modelling the flow of power-law fluids through anisotropic porous media at low pore reynolds number” *Chem. Eng. Sci.* Vol. 61, 2006, pp. 4490-4502.

7. G. Hivet and P. Boisse “Consistent 3D geometrical model of fabric elementary cell. application to a meshing pre-processor for 3d finite element analysis” *Finite Elem. Anal. Design*, Vol. 42, 2005, pp. 25-49.

8. F. Loix, P. Badel, L. Orgéas, C. Geindreau, P. Boisse “Woven fabric permeability: From textile deformation to fluid flow mesoscale simulations” *Compos. Sci. Technol.,* 2008, on line.

9. L. Orgéas, C. Geindreau, J.-L. Auriault, and J.-F. Bloch “Upscaling the flow of generalised newtonian fluids through anisotropic porous media” *J. Non-Newtonian Fluid Mech.* Vol. 145 (2007) pp.15–29.

10. A. Bensoussan, J.-L. Lions, G. Papanicolaou, “*Asymptotic Analysis for Periodic Structures*”, North Holland, Amsterdam, 1978.

11. E. Sanchez-Palencia, “Non-homogeneous media and vibration theory”, *Lectures Notes in Physics*, vol. 127, Springer-Verlag, Berlin, 1980.

12. J.-L. Auriault, “Heterogeneous medium. is an equivalent description possible?” *Int. J. Eng. Sci.* Vol. 29, 1991, pp. 785–795.

13. P. Smith, C.D. Rudd, A.C. Long “The effect of shear deformation on the processing and mechanical properties of aligned reinforcements” *Compos. Sci. Technol.* Vol. 57, 1997, pp 327-344.

14. A. Hammami, F. Trochu, R. Gauvin, S. Wirth “Directional permeability measurement of deformed reinforcement” *J. Reinf. Plast. Compos*. Vol. 15, 1996, pp. 552-562.

15. C.L. Lai, W.B. Young “Model resin permeation of fibre reinforcements after shear deformation” *Polym. Compos.* Vol. 18, 1997, pp. 642-648.

16. J. Slade, E.M. Sozer, S.G. Advani “Fluid Impregnation of deformed preforms” *J. Reinf. Plast. Compos*. Vol. 19, 2000, pp. 552-568.

17. P. Badel, E. Vidal-Salle, E. Maire, P. Boisse “Simulation and tomography analyzis of textile composite reinforcement deformation at the mesoscopic scale”, *Compos. Sci. Technol.* (2008), to appear.